

**INCLINED PULLOUT BEHAVIOUR OF  
ANCHORED GEOGRIDS USED AS VENEER REINFORCEMENT  
IN COVER SYSTEMS OF LANDFILLS**

**RIYA BHOWMIK**



**DEPARTMENT OF CIVIL ENGINEERING  
INDIAN INSTITUTE OF TECHNOLOGY DELHI  
OCTOBER 2019**

**©Indian Institute of Technology Delhi (IITD), New Delhi, 2019**

**INCLINED PULLOUT BEHAVIOUR OF  
ANCHORED GEOGRIDS USED AS VENEER REINFORCEMENT  
IN COVER SYSTEMS OF LANDFILLS**

by

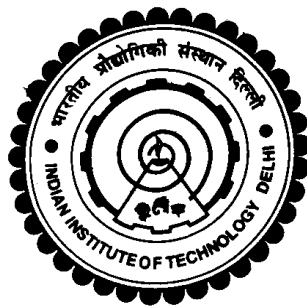
**RIYA BHOWMIK**

**Department of Civil Engineering**

**Submitted**

*in fulfilment of the requirements of the degree of Doctor of Philosophy*

to the



**INDIAN INSTITUTE OF TECHNOLOGY DELHI**

**HAUZ KHAS, NEW DELHI-110016, INDIA**

**OCTOBER 2019**

*To*  
*My Family*

## **CERTIFICATE**

This is to certify that the thesis entitled “**INCLINED PULLOUT BEHAVIOUR OF ANCHORED GEOGRIDS USED AS VENEER REINFORCEMENT IN COVER SYSTEMS OF LANDFILLS**” being submitted by **Ms. Riya Bhowmik** to the **Indian Institute of Technology Delhi** is a record of bonafide research work carried out by her under our supervision and guidance. The thesis work, in our opinion, has reached the standard fulfilling the requirements for **DOCTOR OF PHILOSOPHY** degree. The research report and results presented in this thesis have not been submitted, in part or full, to any University or Institute for the award of any degree or diploma.

**Prof. J.T. Shahu**

Professor

Department of Civil Engineering

Indian Institute of Technology Delhi

New Delhi – 110016

INDIA

**Prof. Manoj Datta**

Professor

Department of Civil Engineering

Indian Institute of Technology Delhi

New Delhi – 110016

INDIA

## ACKNOWLEDGEMENTS

I express my deepest gratitude and indebtedness towards my respected supervisors, **Prof. J.T. Shahu**, and **Prof. Manoj Datta**, Professor, Department of Civil Engineering, Indian Institute of Technology Delhi for their inspiring guidance, painstaking efforts, valuable suggestions, and unfailing support and encouragement throughout this study. I will forever be indebted towards their constant assistance provided during the course of this study. Their volunteered hours of valuable time helped me to put my best efforts in the completion of this study. Their vast knowledge and experience on the subject made this study possible and even more enjoyable.

My sincere thanks to all the faculty members in the Civil Engineering Department, Indian Institute of Technology Delhi for their constant support and encouragement during the entire period of my research work. I also express my sincere thanks to the members of the Student Research Committee, namely, Prof. A. K. Gosain, Prof. G. V. Ramana, and Prof. B. P. Patel for their suggestions during the course of this work.

I am thankful to the staff members of Soil Mechanics, Rock Mechanics, Geology, and Computational laboratories, namely Mr. Manoj Kumar Neelam, Mr. Alok Kumar, Mr. D. Biswas, and Mr. Amit Bundela, respectively, for their cooperation in carrying out the experimental and numerical work. I also extend my thanks to Mr. Amit and Mr. Raju for assisting me with labour work during model tests.

My sincere thanks to my friends and contemporaries, Mrs. Jahnvi Konduru, Ms. Payal Goyal, Dr. Sunita Mishra, Mrs. Mamata Mohanty, Dr. Amit Kumar, Dr. Suresh Kumar, Ms. Aali Pant, Ms. Heena Dhawan, Ms. Kavita Tandon, Ms. Sujata Fulambarkar,

Mrs. Apoorva Agarwal, Mr. Mayuresh Bakare, and Mr. Pranjal Mandhaniya for the support provided during the tenure of this study. I would also like to express my gratitude to all those who have contributed directly or indirectly in the course of my research work.

Last, but certainly not the least, words alone cannot express my deepest gratitude to my parents- Mr. Nitai Charan Bhowmik and Mrs. Jaya Bhowmik, my sisters- Mrs. Rumpa Pal and Dr. Sanghamitra Chatterjee, my brother-in-law Mr. Sanjoy Pal, and my nieces- Srijani and Sreetanuja for their love, constant support, understanding and affection during the tenure of my study that provided me necessary impetus to work on this thesis. It is to my family that this piece of work is gratefully dedicated.

**Riya Bhowmik**

## **ABSTRACT**

The stability of geosynthetics along slopes in covers and liners of landfills depends partly on their mobilized tensile strength and partly on the efficiency of the anchors holding the geosynthetics at the berms or top of the slope. The pull induced on these geosynthetics in the lining or cover system is in an inclined direction parallel to the slope. But due to difficulty in modelling of inclined pullout behaviour experimentally, very few studies have so far been conducted on geosynthetics embedded in anchor trenches and even these studies are limited to sheet-type geosynthetics. For this purpose, an inclined pullout device was conceptualized and developed during the course of this study. This device can perform pullout tests on geosynthetics at continuously varying inclinations.

Since geogrids are widely used as veneer reinforcement, inclined pullout tests are conducted on geogrids embedded in run-out, I-type and L-type anchors in the sand under low confinement. The influence of the angle of inclination of pullout force on the anchor capacity of the geogrid and the variations in the failure mechanism for different types of anchors have been studied. The inclined pullout behaviour has also been studied for sheet geosynthetic embedded in run-out, I-type and L-type anchors under low confinement and compared with the corresponding behaviour of geogrid. For proper comparison, the surface characteristics of the sheet and the geogrid were kept the same by manually fabricating the sheet. The influence of the type of sand on the behaviour of the sheet and the geogrid is also investigated. The results show that the maximum pullout resistance in both the geogrid and the sheet increases by more than 20% as the pull inclination increases from 0° to 30° in all the three types of anchors. In both the sheet and

the geogrid, I-type anchor provides approximately 50% and L-type anchor provides more than 90% higher pullout force than the run-out anchor.

Model tests have also been conducted to investigate the effectiveness of longitudinal and transverse members of the bitumen-coated polyester-yarn geogrids under low normal stress. The tests compare the pullout behaviour of geogrids with different spacing of longitudinal and transverse members. The results show that the spacing between transverse ribs has very little influence on peak pullout resistance of the geogrids, but the residual pullout resistance increases significantly once the transverse rib spacing is greater than a critical value. Increase in spacing between longitudinal ribs reduces the peak pullout resistance considerably.

The model tests on the inclined pullout of geogrids embedded in three types of anchors have been simulated numerically using three-dimensional finite element analyses software PLAXIS 3D. The soil behaviour is represented by the elastic-perfectly plastic Mohr-Coulomb model and the geogrid behaviour with linear-elastic plate elements. The geogrid is modelled using the geometrical and index properties of the geogrid used in model tests. The results show that the peak pullout force values for different values of inclinations and types of anchors were predicted with reasonable accuracy by the numerical modelling approach used in the study. However, the post-peak response for run-out and I-type anchors and the stiffness in case of trench anchors (I- and L-type anchors) are not satisfactorily modelled.

A design formulation to determine the pullout capacity of geosynthetics embedded in run-out, I-type and L-type anchors in sand is proposed. The accuracy of this method is tested by comparing it with the results of the present study and reported results in the literature.

## सार

लैंडफिल के कवर और लाइनर में ढलान के साथ जियोसिंथेटिक्स की संघटित स्थिरता आंशिक रूप से उनकी तन्य शक्ति पर और आंशिक रूप से ढलान के शीर्ष पर जियोसिंथेटिक्स को धारण करने वाले एंकर की दक्षता पर निर्भर करती है। अस्तर या आवरण प्रणाली में इन जियोसिंथेटिक्स पर प्रेरित खिंचाव ढलान के समानांतर एक झुकाव दिशा में आती है। प्रायोगिक रूप से प्रवृत्त पुलआउट व्यवहार के मॉडलिंग में कठिनाई के कारण, अब तक बहुत कम अध्ययनों से लंगर खाई में जियोसिंथेटिक्स पर आयोजित किया गया है और यहां तक कि ये अध्ययन शीट-प्रकार के जियोसिंथेटिक्स तक सीमित हैं। इस उद्देश्य के लिए, इस अध्ययन के दौरान एक प्रवृत्त पुलआउट डिवाइस की अवधारणा और विकास किया गया है। यह उपकरण जियोसिंथेटिक्स पर लगातार अलग-अलग झुकाव पर पुलआउट परीक्षण कर सकता है।

चूंकि जियोग्रिड को व्यापक रूप से लिबास के सुट्टीकरण के रूप में उपयोग किया जाता है, कम खींचा के तहत रेत में रन-आउट, आई-टाइप और एल-प्रकार के एंकर में एम्बेडेड भूगोल पर झुका हुआ पुलआउट परीक्षण किया जाता है। भूगर्भ की लंगर क्षमता पर पुलआउट बल के झुकाव के प्रभाव और विभिन्न प्रकार के लंगर के लिए विफलता तंत्र में भिन्नता का अध्ययन किया गया है। कम खींचतान के तहत रन-आउट, आई-टाइप और एल-टाइप एंकर में एम्बेडेड शीट जियोसिंथेटिक के लिए प्रवृत्त पुलआउट व्यवहार का भी अध्ययन किया गया है और इसकी तुलना जियोग्रिड के संबंधित व्यवहार से की गई है। उचित तुलना के लिए, शीट की सतह की विशेषताओं और जियोग्रिड को शीट को मैनुअल रूप से तैयार करके समान रखा गया था। शीट के व्यवहार और जियोग्रिड पर रेत के प्रकार के प्रभाव की भी जांच की गई है। परिणाम बताते हैं कि जियोग्रिड और शीट दोनों में अधिकतम पुलआउट प्रतिरोध 20% से अधिक बढ़ जाता है क्योंकि सभी तीन प्रकार के एंकरों में पुल झुकाव 0 ° से 30 ° तक बढ़ जाता है। शीट और जियोग्रिड दोनों में, आई-टाइप एंकर लगभग 50% प्रदान करता है और एल-टाइप एंकर रन-आउट एंकर की तुलना में 90% अधिक पुलआउट बल प्रदान करता है।

कम सामान्य तनाव के तहत बिटुमेन-लेपित पॉलिएस्टर-यार्न जॉग्रिड्स के अनुदैर्घ्य और अनुप्रस्थ सदस्यों की प्रभावशीलता की जांच के लिए मॉडल परीक्षण भी किए गए हैं। परीक्षण अनुदैर्घ्य और अनुप्रस्थ सदस्यों के विभिन्न रिक्ति के साथ जियोग्रिड्स के पुलआउट व्यवहार की तुलना करते हैं। परिणाम बताते हैं कि अनुप्रस्थ पसलियों के बीच रिक्ति का जियोग्रिड्स के पीक पुलआउट प्रतिरोध पर बहुत कम प्रभाव पड़ता है, लेकिन एक बार जब ट्रांसवर्स रिब रिक्ति एक महत्वपूर्ण मूल्य से अधिक होती है, तो अवशिष्ट पुलआउट प्रतिरोध बढ़ जाता है। अनुदैर्घ्य पसलियों के बीच रिक्ति में वृद्धि शिखर पुलआउट प्रतिरोध को काफी कम कर देती है।

तीन प्रकार के एंकरों में एम्बेडेड ज्योग्रिड्स के प्रवृत्त पुलआउट पर मॉडल परीक्षणों को तीन आयामी परिमित तत्व विश्लेषण सॉफ्टवेयर PLAXIS 3D का उपयोग करके संख्यात्मक रूप से अनुकरण किया गया है। मृदा व्यवहार लोचदार-पूरी तरह से प्लास्टिक मोहर-कूलम्ब मॉडल और रेखीय-लोचदार प्लेट तत्वों के साथ भूगर्भिक व्यवहार द्वारा दर्शाया गया है। जियोग्रिड को मॉडल परीक्षणों में उपयोग किए जाने वाले जियोग्रिड के ज्यामितीय और सूचकांक गुणों का उपयोग करके मॉडल किया गया है। परिणामों से पता चलता है कि झुकाव के विभिन्न मूल्यों और तीन प्रकार के एंकरों के लिए शिखर पुलआउट बल मूल्यों का अध्ययन में उपयोग किए गए संख्यात्मक मॉडलिंग दृष्टिकोण द्वारा उचित सटीकता के साथ भविष्यवाणी की गई थी। हालांकि, रन-आउट और आई-टाइप एंकर के लिए पोस्ट-पीक प्रतिक्रिया और ट्रेंच एंकर (आई- और एल-टाइप एंकर) के मामले में कठोरता संतोषजनक ढंग से मॉडलिंग नहीं की गई है।

रन-आउट, आई-टाइप और एल-टाइप एंकर में रेत में एम्बेडेड जियोसिंथेटिक्स की पुलआउट क्षमता निर्धारित करने के लिए एक डिजाइन प्रस्तावित किया गया है। इस पद्धति की सटीकता को वर्तमान अध्ययन के परिणामों और साहित्य में रिपोर्ट किए गए परिणामों के साथ तुलना करके परीक्षण किया गया है।

## CONTENTS

	<b>Page No.</b>
<b>Certificate</b>	i
<b>Acknowledgements</b>	iii
<b>Abstract</b>	v
<b>Contents</b>	ix
<b>List of Figures</b>	xvii
<b>List of Tables</b>	xxxix
<b>List of Notations</b>	xxxix
<b>CHAPTER 1 INTRODUCTION</b>	<b>1-15</b>
1.1 General	1
1.2 Landfill Cover Systems	4
1.2.1 Components	4
1.2.2 Geosynthetics in Landfill Cover Systems	6
1.2.3. Stability of Landfill Cover System at Interfaces	7
1.2.4. Anchorage of Veneer Reinforcement	7
1.3 Need for the Present Study	9
1.4 Objectives	10
1.5 Scope and Methodology	11
1.5.1. Development of New Inclined Pullout Apparatus	11

1.5.2.	Model Tests	12
1.5.3.	Finite Element Analysis	12
1.6	Organisation of Thesis	13
<b>CHAPTER 2      LITERATURE REVIEW</b>		<b>17-54</b>
2.1	General	17
2.2	Landfill Cover Systems	17
2.2.1	Components of Landfill Cover Systems	17
2.2.2	Geosynthetics in Landfill Cover Systems	20
2.2.3.	Interfaces in Landfill Cover Systems	24
2.2.4	Veneer Reinforcement	26
2.3	Stability Analysis	30
2.3.1	Veneer Reinforcement in Landfill Cover Systems	30
2.3.2	Anchorage of Veneer Reinforcement	35
2.4	Model Tests	41
2.4.1.	Horizontal Pullout of Geosynthetics	41
2.4.2.	Inclined Pullout of Geosynthetics	47
2.5	Numerical Analysis	50
2.5.1	Horizontal Pullout of Geosynthetics	50
2.5.2	Inclined Pullout of Geosynthetics	52
2.6	Research Gaps	53

<b>CHAPTER 3</b>	<b>VARIABILITY IN ANCHORAGE</b>	<b>55-61</b>
	<b>CAPACITIES: COMPARISON OF</b>	
	<b>EXISTING METHODS</b>	
3.1	General	55
3.2	Analysis	55
3.3	Results	58
3.4	Conclusions	61
<b>CHAPTER 4</b>	<b>DEVELOPMENT OF AN IMPROVED</b>	<b>63-82</b>
	<b>INCLINED PULLOUT DEVICE</b>	
4.1	General	63
4.2	Conceptual Development Procedure	64
4.3	New Inclined Pullout Device	65
4.3.1	Pullout and Inclination System	67
4.3.1.1.	Inclined Pulling Unit	67
4.3.1.2.	Vertical Positioning Unit	67
4.3.1.3.	Horizontal Positioning Unit	68
4.3.2	Test Tank	79
4.4	Summary	82
<b>CHAPTER 5</b>	<b>EXPERIMENTAL INVESTIGATIONS</b>	<b>83-102</b>
5.1	General	83
5.2	Materials	83
5.2.1	Yamuna Sand	83

5.2.2	Badarpur Sand	87
5.2.3	Geogrids	87
5.3	Testing Programme	94
5.4	Testing Procedure	96
5.4.1	Horizontal and Inclined Pullout Tests on Run-out Anchors	96
5.4.2	Horizontal and Inclined Pullout Tests on I-type and L-type anchors	99
<b>CHAPTER 6</b>	<b>HORIZONTAL AND INCLINED PULLOUT BEHAVIOUR OF GEOGRIDS ANCHORED IN TRENCHES</b>	<b>103-136</b>
6.1	General	103
6.2	Repeatability of Results	106
6.3	Anchors under Horizontal Pull	109
6.4	Influence of Inclination on Pullout Capacity	114
6.5	Influence of Type of Sand	118
6.6	Comparison with Experimental Results Reported in Literature	122
6.7	Comparison of Experimental Results with Predicted Values by Analytical Methods	125
6.8	Conclusions	135

<b>CHAPTER 7</b>	<b>HORIZONTAL AND INCLINED PULLOUT</b>	<b>137-162</b>
	<b>BEHAVIOUR OF GEOSYNTHETIC SHEET</b>	
	<b>VIS-À-VIS GEOGRID</b>	
7.1	General	137
7.2	Repeatability of Results	138
7.3	Anchors under Horizontal Pull	142
7.4	Influence of Inclination of Pullout Force	147
7.5	Influence of Type of Sand	149
7.6	Comparison with Analytical Methods	154
7.7	Conclusions	161
<b>CHAPTER 8</b>	<b>INFLUENCE OF SPACING OF</b>	<b>163-187</b>
	<b>TRANSVERSE AND LONGITUDINAL</b>	
	<b>MEMBERS AND APERTURE SIZE OF</b>	
	<b>GEOGRID ON PULLOUT RESPONSE OF</b>	
	<b>RUN-OUT ANCHORS</b>	
8.1	General	163
8.2	Repeatability of Results	170
8.3	Influence of Variation of Spacing between Transverse Ribs	171
8.4	Influence of Variation of Spacing between Longitudinal Ribs	178

8.5	Influence of Variation of Aperture Size	183
8.6	Conclusions	186
<b>CHAPTER 9 FINITE ELEMENT ANALYSIS OF MODEL TESTS</b>		<b>189-222</b>
9.1	General	189
9.2	Numerical Modelling	190
9.2.1.	PLAXIS 3D Software Package	190
9.2.2	Modelling of Components	190
9.2.2.1.	Modelling of Geogrid	192
9.2.2.2.	Modelling of Soil	195
9.2.2.3	Interfaces	197
9.2.3.	Boundary Conditions and Prescribed Displacement	199
9.2.4.	Mesh Sensitivity Analysis	199
9.2.5.	Computation and Convergence Criteria	201
9.3	Results and Discussion	201
9.3.1.	Horizontal Pullout of Geogrids in Run-out Anchor	201
9.3.2.	Inclined Pullout of Geogrids in Run-out Anchor	205
9.3.2.1.	‘Geogrid’ element versus ‘Plate’ element	205
9.3.2.2.	Influence of length of the clamp in numerical simulation	208
9.3.2.3.	Influence of inclination of pullout force	210

9.3.3. Horizontal and Inclined Pullout of Geogrids in I- and L-type anchors	211
9.3.3.1. I-type anchor	211
9.3.3.2. L-type anchor	216
9.4 Conclusions	220
<b>CHAPTER 10 PROPOSED IMPROVEMENT IN ESTIMATION OF PULLOUT RESISTANCE OF VENEER REINFORCEMENT IN ANCHOR TRENCHES</b>	<b>223-237</b>
10.1 General	223
10.2 Evaluation of Modification Factor	225
10.3 Evaluation of Anchorage Capacity Based on Proposed Methodology	230
10.4 Summary	236
<b>CHAPTER 11 CONCLUSIONS AND SUGGESTIONS FOR FUTURE RESEARCH</b>	<b>239-245</b>
11.1 General	239
11.2 Conclusions	240
11.3 Suggestions for Future Research	245
<b>REFERENCES</b>	<b>247-259</b>
<b>CURRICULUM VITAE</b>	<b>261-265</b>

**LIST OF FIGURES**

<b>Fig. No.</b>	<b>Description</b>	<b>Page No.</b>
1.1	Impact of the waste dump on the environment.	2
1.2	(a) Nearly vertical configuration of the slope of a waste dump in Ghazipur, Delhi, (b) Steep configuration of the slope of a waste dump in Okhla, Delhi, (c) Steep configuration of the slope of a waste dump in Bhalswa, Delhi.	3
1.3	Components of MSW cover system and minimum specifications by MoEF&CC in India (MoEF&CC 2016).	5
1.4	Components of HW cover system and minimum specifications by CPCB in India (CPCB 2001).	5
1.5	Use of geosynthetics in landfill cover system.	6
1.6	Forces acting on a geogrid-reinforced cover system.	7
1.7	Anchorage of veneer reinforcement.	8
1.8	(a) Run-out anchor, (b) I-type anchor, (c) L-type anchor, (d) U-type anchor, (e) V-type anchor.	8
2.1	Case History of veneer stability in Connecticut, USA (Carroll and Chouery-Curtis 1991).	26
2.2	Cover system of HW landfill reinforced with geogrids in Fullerton, California, USA (Zornberg 2005).	27

2.3	(a) Schematic view of the cover system of MSW landfill reinforced with geocell and geogrid in Ghazipur, Delhi, India (Datta 2014), (b) Laying of Geocells over Geogrid for cover system of Ghazipur landfill, (c) Vegetative cover on Geocell layer of cover system of Ghazipur landfill.	28
2.4	Anchorage of geogrids in the cover system of Ghazipur landfill (Datta 2014).	29
2.5	Limit Equilibrium forces associated with Infinite Slope Analysis method.	31
2.6	Limit equilibrium forces associated with two-wedge methods.	32
2.7	(a) I-type anchor, (b) L-type anchor.	36
2.8	(a) Stresses at the interface considered by Hullings & Sansone (1998), (b) Stresses at the interface considered by Koerner (2005), (c) Stresses at the interface considered by Qian et al. (2002), (d) Stresses at the interface considered by Villard and Chareyre (2004).	37
2.9	Schematic Diagram of Experimental Set-Up as per ASTM D6706-01.	47
2.10	(a) Photograph of the inclined pull-out apparatus by Koerner and Wayne (1991), (b) Schematic diagram of Experimental Set-up by Koerner and Wayne (1991).	48
2.11	Schematic Diagram of Experimental Set-Up developed by Chareyre et. al. (2002).	48
2.12	Extraction of geotextile layer embedded in (i) and (ii) L-shaped anchor trench and (iii) and (iv) V-shaped anchor trench (from Girard et al. 2006).	49

3.1	Landfill cover system with the run–out anchor.	57
3.2	Landfill cover system with the I-type anchor.	57
3.3	Landfill cover system with the L-type anchor.	57
3.4	Comparison of $T_{\text{anchor}}$ obtained from different methods for run-out anchor.	58
3.5	Comparison of $T_{\text{anchor}}$ obtained from different methods for I-type anchor.	59
3.6	Comparison of $T_{\text{anchor}}$ obtained from different methods for L-type anchor.	59
4.1	Steps of development of design of the new inclined pullout device.	66
4.2	(a) The schematic perspective view of the pullout device set for horizontal pullout, (b) The schematic side view of the device set for horizontal pullout, (c) The schematic perspective view of the device set for inclined pullout, (d) The schematic side view of the device set for inclined pullout, (e) The schematic perspective view of the components for inclined pullout, (f) The schematic perspective view of the components of pulling arm.	69
4.3	(a) Photograph of the device during inclined pull, (b) Photograph of components for inclined pullout.	78
4.4	(a) Schematic half-model representation of arrangement of geogrid in run-out anchor in test tank, (b) Schematic half-model representation of arrangement of geogrid in I-type anchor in test tank, (c) Schematic half-model representation of arrangement of geogrid in L-type anchor in test tank.	80

---

4.5	(a) Test tank setup for 0° inclination, (b) Test tank setup for 25° inclination.	81
5.1	Particle size distribution of Yamuna and Badarpur sand.	84
5.2	Different stages to extract morphological characteristics of sand particles of Badarpur sand using Image-J.	86
5.3	(a) X-ray diffraction result of Yamuna sand, (b) X-ray diffraction result of Badarpur sand.	86
5.4	Original Geogrid Specimen.	88
5.5	(a) Axial force-strain result from wide-width tensile test of geogrid in machine-direction, (b) Axial force-strain results from tensile tests on longitudinal and transverse ribs of geogrid.	89
5.6	Tensile test equipment: wide-width tensile test in progress.	91
5.7	3D Optical Profilometer.	92
5.8	Analysis of surface roughness of geogrid: (a) Close view of junction of longitudinal and transverse ribs, (b) Surface Profile of Section A on longitudinal rib, (c) Surface Profile of Section B on transverse rib, (d) Surface Profile of Section C on junction.	92
5.9	Test tank setup for 25° inclination.	97
5.10	Photograph of the device during inclined pull.	98
5.11	(a) Construction of I-type anchor in sand using T-shape board, (b) Construction of L-type anchor in sand using T-shape board, (c) Untying of tie-ropes while filling of sand, (d) Lifting of T-shape board, (e) Laying of the horizontal part of the geogrid, (f) Final compacted sand bed.	100

6.1	(a) Runout anchor (RO L80), (b) I-type anchor (AT L60 D20), (c) L-type anchor (AT L40 D20 B20).	104
6.2	(a) Repeatability of pullout force-displacement relationship in run-out anchor under the horizontal pull, (b) Repeatability of pullout force-displacement relationship in I-type anchor under horizontal pull, (c) Repeatability of pullout force-displacement relationship in L-type anchor under horizontal pull, (d) Repeatability of maximum pullout force for run-out anchor for pull under three different inclinations.	107
6.3	Pullout force-displacement relationships for three types of anchor under horizontal pull.	110
6.4	Pullout force-displacement relationships for three types of anchor under 15° inclined pull.	111
6.5	Pullout force-displacement relationships for three types of anchor under 25° inclined pull.	112
6.6	Top view of the test tank showing the extent of the displaced top soil after each case of pullout test: (a) Geogrid in run-out anchor, (b) Geogrid anchored in I-type anchor, (c) Geogrid anchored in L-type anchor.	112
6.7	(a) Comparison of maximum pullout force for run-out anchor under inclined pull, (b) Comparison of maximum pullout force for I-type anchor under inclined pull, (c) Comparison of maximum pullout force for L-type anchor under inclined pull.	115
6.8	(a) Comparison of pullout force values at large displacement for run-out anchor under inclined pull, (b) Comparison of pullout force values at large displacement for I-type anchor under inclined pull, (c) Comparison of pullout force values at large displacement for L-type anchor under inclined pull.	117

6.9	(a) Comparison of pullout load-displacement relationships for run-out anchor under horizontal pull for geogrid in Yamuna sand and Badarpur sand, (b) Comparison of pullout load-displacement relationships for I-type anchor under horizontal pull for geogrid in Yamuna sand and Badarpur sand, (c) Comparison of pullout load-displacement relationships for L-type anchor under horizontal pull for geogrid in Yamuna sand and Badarpur sand.	119
6.10	(a) Comparison of maximum pullout resistance of geogrid in run-out anchor in Yamuna and Badarpur sand under varying inclinations of pull, (b) Comparison of maximum pullout resistance of geogrid in I-type anchor in Yamuna and Badarpur sand under varying inclinations of pull, (c) Comparison of maximum pullout resistance of geogrid in L-type anchor in Yamuna and Badarpur sand under varying inclinations of pull.	121
6.11	(a) Comparison of experimental test results with Chareyre et al. (2002) model test results for run-out anchor under varying inclinations of pullout force, (b) Comparison of experimental test results with Chareyre et al. (2002) model test results for different anchors under 20° inclined pull.	123
6.12	(a) Conceptualized pullout interaction mechanism for geosynthetic under low normal stress-side view, (b) Idealized pullout interaction mechanism for geosynthetic under low normal stress -perspective view.	126
6.13	Comparison of measured maximum pullout force in experiments with the predicted results.	127
6.14	Schematic of the model used by Shahu (2007) for developing a mechanistic formulation.	133
6.15	Comparison of experimental test results of run-out anchor with Shahu (2007) model.	134
7.1	(a) Original Geogrid Specimen, (b) Sheet prepared from ribs of	138

	geogrid specimen.	
7.2	(a) Repeatability in pullout force-displacement relationship in sheet run-out anchor under horizontal pull in Yamuna sand, (b) Repeatability in pullout force-displacement relationship in sheet I-type anchor under horizontal pull in Yamuna sand, (c) Repeatability in pullout force-displacement relationship in sheet L-type anchor under horizontal pull in Yamuna sand.	139
7.3	Repeatability in maximum pullout resistance for sheet run-out anchor under pull at three different inclinations in Yamuna sand.	141
7.4	Repeatability of maximum pullout force for three different types of anchors under horizontal pull in Badarpur sand.	141
7.5	Pullout load-displacement relationships for three types of sheet anchor under horizontal pull in Yamuna sand.	143
7.6	(a) Pullout load-displacement relationships of sheet and geogrid runout anchor under horizontal pull in Yamuna sand, (b) Pullout load-displacement relationships of sheet and geogrid I-type anchor under horizontal pull in Yamuna sand, (c) Pullout load-displacement relationships of sheet and geogrid L-type anchor under horizontal pull in Yamuna sand.	144
7.7	Top view of the test tank showing the extent of the displaced top soil after each case of pullout test: (a) Sheet in run-out anchor, (b) Sheet anchored in I-type anchor, (c) Sheet anchored in L-type anchor.	146
7.8	Comparison of maximum pullout resistance of geogrid and sheet runout anchor under varying inclinations of pull.	147
7.9	(a) Pullout load-displacement relationships of sheet and geogrid run-out anchor under 10° inclined pull in Yamuna sand, (b) Pullout load-displacement relationships of sheet and geogrid run-out anchor under 20° inclined pull in Yamuna sand.	148

7.10	(a) Comparison of Pullout load-displacement relationships for run-out anchor under horizontal pull for Geogrid and Sheet in Badarpur sand, (b) Comparison of Pullout load-displacement relationships for I-type anchor under horizontal pull for Geogrid and Sheet in Badarpur sand, (c) Comparison of Pullout load-displacement relationships for L-type anchor under horizontal pull for Geogrid and Sheet in Badarpur sand.	150
7.11	Top view of the test tank showing the extent of the displaced top soil after each case of pullout test in Badarpur sand: (a) Sheet anchored in run-out anchor, (b) Sheet anchored in L-type anchor.	151
7.12	(a) Comparison of maximum pullout force for three types of sheet and geogrid anchor in Yamuna and Badarpur sand under horizontal pull, (b) Comparison of maximum pullout resistance of sheet and geogrid run-out anchor in Yamuna and Badarpur sand under varying inclinations of pull.	152
7.13	Comparison of maximum pullout resistance of geogrid embedded in three types of anchor in Yamuna and Badarpur sand under varying inclinations of pullout force.	153
7.14	Comparison of measured maximum pullout force in experiments with the predicted results for Sheet.	155
7.15	(a) Comparison of measured maximum pullout force for sheet embedded in different anchors under horizontal pullout with the predicted results for Badarpur Sand, (b) Comparison of measured maximum pullout force for sheet and geogrid in run-out anchor under different inclinations with the predicted results for Badarpur Sand, (c) Comparison of measured maximum pullout force for geogrid in I-type anchor under different inclinations with the predicted results for Badarpur Sand, (d) Comparison of measured maximum pullout force for geogrid in L-type anchor under different inclinations with the predicted results for Badarpur Sand.	156

---

7.16	Variation of non-dimensional pullout force factor $P^*$ with varying inclinations of pullout force (Patra and Shahu 2012).	159
7.17	Comparison of experimental test results of run-out anchor with Shahu (2007) and Patra and Shahu (2012) models.	160
8.1	Schematic diagram of the pullout tests.	164
8.2	Geogrid specimens with varying aperture sizes in the longitudinal direction due to removal of T-ribs: (a) Original Geogrid (GG): T-rib spacing – 18 mm, L-rib spacing – 20 mm, (b) 40 mm (T4), (c) 60 mm (T6), (d) 80 mm (T8), (e) 100 mm (T10), (f) 120 mm (T12), (g) 140 mm (T14), (h) 400 mm (T40), (i) 800 mm (T80).	165
8.3	Geogrid specimens with varying aperture sizes in the transverse direction due to removal of L-ribs: (a) Original Geogrid (GG): T-rib spacing – 18 mm, L-rib spacing – 20 mm, (b) 45 mm (L4), (c) 70 mm (L7), (d) 95 mm (L9), (e) 140 mm (L14).	167
8.4	Fig. 7 Geogrid specimens with varying aperture sizes in both longitudinal and transverse direction due to removal of both L-ribs and T-ribs: (a) Original Geogrid (GG): T-rib spacing – 18 mm, L-rib spacing – 20 mm, (b) 45 mm (LT4), (c) 70 mm (LT7), (d) 95 mm (LT9).	169
8.5	(a) Repeatability in pullout force-displacement behaviour of T12 and T80 geogrids, (b) Repeatability in pullout force-displacement behaviour of L4 and L14 geogrids.	170
8.6	Pullout force-displacement behaviour of geogrids with varying distance between T-ribs.	173
8.7	Comparison of maximum and residual pullout resistance of geogrids with varying spacing between T-ribs.	173

8.8	(a) Top view of the test tank showing the extent of the displaced top soil after pullout test of GG, (b) Top view of the test tank showing the extent of the displaced top soil after pullout test of T4, (c) Top view of the test tank showing the extent of the displaced top soil after pullout test of T14, (d) Top view of the test tank showing the extent of the displaced top soil after pullout test of T80.	174
8.9	(a) Pullout force-displacement relationships of single rib and multiple ribs with varying spacing between them, (b) Comparison of normalized peak pullout force values of multiple L-ribs at 20 mm spacing with that of single rib pullout capacity, (c) Comparison of normalized peak pullout force values of two L-ribs with varying spacing with that of single rib pullout capacity.	177
8.10	(a) Pullout force-displacement behaviour of geogrids with varying spacing between L-ribs, (b) Comparison of maximum and residual pullout resistance of geogrids with varying spacing between L-ribs.	180
8.11	Normalized Pullout force-displacement response of geogrids with varying spacing between L-ribs.	181
8.12	(a) Top view of the test tank showing the extent of the displaced top soil after pullout test of L4, (b) Top view of the test tank showing the extent of the displaced top soil after pullout test of L9.	182
8.13	(a) Pullout force-displacement behaviour of geogrids with varying spacing between T-ribs and L-ribs, (b) Comparison of maximum and residual pullout resistance for geogrids with varying spacing between T-ribs and L-ribs.	184
8.14	Normalized Pullout force-displacement response for geogrid specimens with varying spacing between L-ribs.	185

9.1	Complete 3D mesh geometry of the FE model of geogrid in three types of anchor.	191
9.2	(a) Modelling of geogrid with longitudinal rib as ‘Geogrid’ element, (b) Modelling of geogrid with longitudinal rib as ‘Plate’ element.	192
9.3	(a) Modelling of geogrid in I-type Anchor, (b) Modelling of geogrid in L-type Anchor.	193
9.4	Pullout force-displacement results from numerical modelling of horizontal pullout of geogrid with different values of $R_{inter}$ .	198
9.5	(a) Pullout force-displacement results from numerical modelling of horizontal pullout of geogrid with different element sizes, (b) Pullout force-displacement results from finite element modelling of horizontal pullout of geogrid with different values of tolerance error.	200
9.6	Comparison of experimental results under horizontal pullout with finite element results for GG1 and GG2 models.	203
9.7	(a) Top soil movement during model test on geogrid embedded in run-out anchor, (b) Top soil movement in GG1 model, (c) Top soil movement in GG2 model.	203
9.8	Displacement at the rear-end of the geogrid in run-out anchor with respect to the front-end under horizontal pullout.	205
9.9	Comparison of experimental results under 20° inclined pullout with finite element results for GG1 and GG2 models.	206
9.10	(a) Deformation of the geogrid under 20° inclined pullout for GG1 model, (b) Deformation of the geogrid under 20° inclined pullout for GG2 model.	207

---

9.11	(a) Comparison of experimental result under 20° inclined pullout with finite element results for varying clamp length, (b) Effect of clamp length on horizontal and vertical components of pullout force under 20° inclined pull.	209
9.12	Comparison of maximum pullout resistance of geogrid obtained from experiments and FE model under varying inclinations of pull.	210
9.13	Comparison of experimental results for pullout of geogrid in I-type anchor with the predicted results from numerical modelling with different values of $R_{inter}$ and under varying inclinations of pullout force.	212
9.14	Deformation of geogrid in I-type anchor in finite element analysis.	214
9.15	Schematic representation demonstrating the difference in deformation of the vertical part of the geogrid embedded in trench in numerical analysis with respect to experiment.	215
9.16	(a) Comparison of experimental results for horizontal pullout of geogrid in L-type anchor with the predicted results from numerical modelling with different values of $R_{inter}$ , (b) Comparison of peak pullout resistance in L-type anchor with the predicted values from numerical modelling with different values of $R_{inter}$ and under varying inclinations of pullout force.	216
9.17	Deformation of geogrid in L-type anchor in finite element analysis.	219
9.18	Comparison of measured maximum pullout resistance of geogrid embedded in run-out, I-type and L-type anchors from experiments with the predicted results from finite element analyses under varying inclinations of pull.	220
10.1	Euler-Eytelwein belt friction model (Thiel 2010).	224

10.2	Stress state at the interface for run-out anchor.	225
10.3	Stress state at the interface for I-type anchor.	226
10.4	Stress state at the interface for L-type anchor.	227
10.5	Correlation of modification factor for weighting coefficient with varying inclinations of pullout force.	229
10.6	(a) Comparison of measured maximum pullout force values for sheet in run-out anchor in Yamuna sand (YS) with the predicted values by the proposed and VC-i formulations, (b) Comparison of measured maximum pullout force values for sheet in run-out anchor in Badarpur sand (BS) with the predicted values by the proposed and VC-i formulations.	231
10.7	(a) Comparison of measured maximum pullout force values for geogrid in run-out anchor in Yamuna sand with the predicted values by the proposed and VC-i formulations, (b) Comparison of measured maximum pullout force values for geogrid in run-out anchor in Badarpur sand with the predicted values by the proposed and VC-i formulations.	232
10.8	(a) Comparison of measured maximum pullout force values for geogrid in I-type anchor in Yamuna sand with the predicted values by the proposed and VC-i formulations, (b) Comparison of measured maximum pullout force values for geogrid in I-type anchor in Badarpur sand with the predicted values by the proposed and VC-i formulations.	233
10.9	(a) Comparison of measured maximum pullout force values for geogrid in L-type anchor in Yamuna sand with the predicted values by the proposed and VC-i formulations, (b) Comparison of measured maximum pullout force values for geogrid in L-type anchor in Badarpur sand with the predicted values by the proposed and VC-i formulations.	234

- 10.10 (a) Comparison of model test results by Chareyre et al. (2002) for run-out anchor under varying inclinations of pullout force with the predicted values by the proposed and VC-i formulations, (b) Comparison of model test results by Chareyre et al. (2002) for different anchors under 20° inclined pull with the predicted values by the proposed and VC-i formulations. 235

**LIST OF TABLES**

<b>Fig. No.</b>	<b>Description</b>	<b>Page No.</b>
2.1	Components of the cover system and minimum specifications by regulatory agencies of India, US and Germany.	19
2.2	Types and functions of geosynthetics used in landfills (Bouazza et.al. 2002).	21
2.3	Range of peak interface shear strength parameters obtained from tests conducted under dry conditions reported in the literature.	25
2.4	Summary of literature for two-wedge analysis methods on slope stability of the cover.	34
2.5	Summary of literature on design methods of anchorage capacity.	40
2.6	Summary of Horizontal & Inclined Pullout Test Apparatus.	42
3.1	Soil Properties.	56
4.1	Details of Components of the Inclined Pullout Device.	75
5.1	Properties of sand.	85
5.2	Properties of geogrid.	88
5.3	Results obtained from wide-width tensile tests performed on all specimens of geogrid in machine-direction.	90

5.4	Summary of Model Tests on Geogrids (Chapter 6).	94
5.5	Summary of Model Tests on Sheet and Geogrid (Chapter 7).	95
5.6	Summary of Model Tests on Geogrids with various spacing between its ribs (Chapter 8).	95
6.1	Details of Model Tests.	105
6.2	Comparison of measured maximum pullout force under different inclinations in experiments with the predicted results.	130
8.1	Properties of geogrid with variation of spacing between L-ribs.	179
9.1	Material properties of ‘Geogrid’ and ‘Plate’ elements considered in the analysis.	195
9.2	Material properties of soil considered in the analysis .	196
9.3	Variation in values of Young’s modulus of Yamuna sand with confining pressure.	197
10.1	Modification factor for weighting coefficients with varying inclinations of pullout force.	229

## **LIST OF NOTATIONS**

1D	One-Dimensional (analysis)
2D	Two-Dimensional (analysis)
3D	Three-Dimensional (analysis)
A	Area of the Particle
ASTM	American Society for Testing and Materials
AT	Anchor Trench
B	Width of the Anchor Trench
$B_g$	Width of the geosynthetic reinforcement in anchor
BS	Badarpur Sand
c	Cohesion intercept of soil
$c_A$	Adhesive force between cover soil of the active wedge and the geosynthetic
$C_c$	Coefficient of Curvature of particle size distribution of soil
CCL	Compacted Clay Liner
CSPE-R	Reinforced Chlorosulfonated Polyethylene
$C_u$	Coefficient of Uniformity
d	Thickness of the 'Plate' element in PLAXIS
D	Depth of Anchor Trench
$D_{10}$	Particle size (diameter) at which 10 percent of the soil is finer
$D_{50}$	Particle size (diameter) at which 50 percent of the soil is finer
$D_{85}$	Particle size (diameter) at which 85 percent of the soil is finer
DEG	Degree of Inclination of Pullout Force

DEM	Discrete Element Method
E	Young's modulus
$E_A$	Inter-wedge force acting on active wedge from passive wedge
$E_P$	Inter-wedge force acting on passive wedge from active wedge
ERF	Enhanced Resisting Force
$f_b$	The bond coefficient between soil and geosynthetic
FEA	Finite Element Analysis
FEM	Finite Element Method
FS	Factor of Safety
GCL	Geosynthetic Clay Liner
GG1 model	Numerical model in which the longitudinal ribs of the geogrid are modelled with axial element and the transverse ribs of the geogrid are modelled with bending element.
GG2 model	Numerical model in which both the longitudinal ribs and transverse of the geogrid are modelled with bending element.
GG-E	Experimental peak pullout resistance of geogrid
GG-GS-P	Predicted peak pullout resistance of geogrid using general failure mechanism
GG-LS-P	Predicted peak pullout resistance of geogrid using Prandtl local shear failure mechanism
GG-mPS-P	Predicted peak pullout resistance of geogrid using modified punching failure mechanism
GG-PS-P	Predicted peak pullout resistance of geogrid using punching failure mechanism
GM	Geomembrane
H	Thickness of overburden
H:V	Horizontal: Vertical indicating inclination of slope

H'	Height between berms
HDPE	High-Density Polyethylene
HS	Hullings and Sansone (1998) method
ISA	Infinite slope analysis method
J	Secant modulus of the geosynthetic in kN/m
J*	Ratio of the reinforcement stiffness to the axial pullout capacity
k	Coefficient of Permeability, m/s
K <sub>a</sub>	Coefficient of active earth pressure
K <sub>o</sub>	Coefficient of earth pressure at rest
K <sub>oe</sub>	Koerner (2005) method
K <sub>p</sub>	Coefficient of passive earth pressure
K <sub>1</sub>	Weighting Coefficient for increase in slip resistance at bends for inclination < 90° in run-out anchor
K <sub>2</sub>	Weighting Coefficient for increase in slip resistance at bends for inclination = 90° in I-type anchor
K <sub>3</sub>	Weighting Coefficient for increase in slip resistance at bends for inclination = 90° in L-type anchor
K <sub>new</sub>	Weighting Coefficient for increase in slip resistance at bends in proposed design formulation
L	Run-out length of the reinforcement
L <sub>r</sub>	Total length of the geosynthetic in anchors
L-ribs	Longitudinal ribs of geogrid
LT-specimens	Specimens in which the spacing between both longitudinal and transverse ribs is varied simultaneously.
M <sub>1</sub>	Modification factor for weighting coefficient K <sub>1</sub>
M <sub>2</sub>	Modification factor for weighting coefficient K <sub>2</sub>

$M_3$	Modification factor for weighting coefficient $K_2$ and $K_3$
$M$	Modification factor for weighting coefficient in the proposed design formulation
$N$	Effective force normal to the failure plane
$N_A$	Normal effective force of active wedge
$N_P$	Normal effective force of passive wedge
$P$	Perimeter of the Particle
$P_{r-bottom}$	Interface shear resistance at the bottom of the geosynthetic during pullout
$P_{rg}$	Pullout resistance of geogrids
$P_{rgb}$	Bearing resistance at the transverse ribs of the geogrid
$P_{rs}$	Pullout resistance of sheet
$P_{r-sides}$	Frictional resistance on the back and sides of the geosynthetic during pullout
PVC	Polyvinyl Chloride
QKG	Qian et al. (2002) method
RAM	Random Access Memory
Res.	Residual pullout resistance of geosynthetic
$R_{inter}$	Strength-reduction factor used to model the behaviour of interface elements in PLAXIS.
RO	Run-out
$S$	Spacing between transverse ribs of the geogrid
Sheet-E	Experimental peak pullout resistance of sheet
Sheet-P	Predicted peak pullout resistance of sheet
SP	Poorly graded sand
$t$	Thickness of cover soil, m

T	Long-term Design Strength of Geosynthetics, in kN/m
T1	Anchorage Capacity of veneer reinforcement
T <sub>Experiment</sub>	Pullout capacity of the anchor obtained from model test
t <sub>g</sub>	Thickness of the transverse rib of the geogrid
T-ribs	Transverse ribs of geogrid
VC	Villard and Chareyre (2004) method
VC-i	Villard and Chareyre (2004) method when pullout failure occurs at the interface
VC-s	Villard and Chareyre (2004) method when pullout failure occurs in soil
VFPE	very flexible polyethylene
W	Weight of cover soil
W <sub>A</sub>	Weight of active wedge
W <sub>P</sub>	Weight of passive wedge
YS	Yamuna Sand
$\alpha_b$	Total frontal area available for bearing resistance
$\alpha_s$	Fraction of geogrid solid area
$\beta$	Inclination of Slope
$\gamma$	Unit Weight of Soil
$\delta$	Angle of shearing resistance at the soil-geosynthetic or geosynthetic-geosynthetic interfaces
$\nu$	Poisson's ratio
$\sigma_b$	Bearing stress mobilized on transverse ribs
$\sigma_n$	Normal stress on the reinforcement
$\phi$	Angle of shearing resistance of soil
$\psi$	Dilatancy angle